Supporting information:

Cocrystallization Tailoring Radiative Decay Pathways for Thermally Activated Delayed Fluorescence and Room Temperature Phosphorescence emission

Kun Liu,[a,§] Shuai Li,[a,§] Liyuan Fu,[b] Yilong Lei,[c] Qing Liao,*[b] Hongbing Fu*[a,b]

[a] *Institute of Molecule Plus (IMP), School of Engineering and Technology, Tianjin University, Tianjin, 300072, China.*

[b] *Beijing Key Laboratory for Optical Materials and Photonic Devices, Department of Chemistry, Capital Normal University, Beijing, 100048，China.*

[c] *Department of Chemistry, School of Science, Tianjin University, Tianjin, 300072，China.*

*Corresponding Author: liaoqing@cnu.edu.cn; hbfu@cnu.edu.

§ These authors contributed equally to this work.

Keywords: excited state processes, thermally activated delayed fluorescence, room temperature phosphorescence, charge-transfer cocrystals, heavy-atom effect

Table of Contents

Experimental Details

Materials and chemicals: Dibenzothiophene (DBT), 2-bromodibenzo[b,d]thiophene (2-BrDBT), 3-bromodibenzo[b,d]thiophene (3-BrDBT), 4-bromodibenzo[b,d]thiophene (4-BrDBT), and 1,2,4,5-tetracyanobenzene (TCNB) were purchased from TCI. And, tetrahydrofuran (THF, HPLC) acetonitrile (HPLC), ethanol absolute (HPLC) and isopropanol (HPLC) were purchased from Tianjin Chemical Agent. Ultrapure water with a resistivity of 18.2 MΩ•cm^{-1} was obtained by using a Milli-Q apparatus (Milipore). All of them were directly used without further purification (Fig. S15-19).

Synthesis of 2-, 3- and 4-BrTC microrods: 1D TCNB-based CT microrods 2-, 3- and 4-BrTC were synthesized by a CT-directed assembly route. Typically, 0.5 mL of an electron donor solution (2-BrDBT, 3-BrDBT or 4-BrDBT) in THF was first mixed with 0.5 mL of an electron acceptor solution (TCNB) in THF in an equimolar concentration ($C_{2\text{-BrDBT}} = C_{3\text{-BrDBT}} = C_{4\text{-BrDBT}} = C_{TCNB}$ = 40 mM). The two mixed solutions were allowed to stand for several minutes for the formation of stable binary CT complexes. And then, 1 mL of the mixture solution was injected slowly into 5 mL of an isopropanol /H_2O mixture (v/v = 3:2) to induce the formation of 2-BrTC, 3-BrTC or 4-BrTC microstructures. Finally, the suspension was directly dropped onto the substrate and then the 1D CT assemblies were left upon the solvents were completely removed.

Synthesis of DTC microrods: Similarly, DTC microrods were also prepared by a CT-directed assembly route. Typically, 0.5 mL of an electron donor solution (DBT) in acetonitrile was mixed with 0.5 mL of an electron acceptor solution (TCNB) in acetonitrile with equimolar concentration ($C_{DBT} = C_{TCNB}$ =20 mM). The mixed solutions were allowed to stand for several minutes for the formation of stable binary CT complexes. And then, 1 mL of a CT mixed solution was injected slowly into 5 mL of an ethanol/H_2O mixture (v/v =2:3) to induce the formation of DTC.

Sample characterization: The morphologies and sizes of the two CT assemblies were examined using field-emission scanning electron microscopy (SEM, Hitachi S4800) at an acceleration voltage of 5 kV. Transmission electron microscopy (TEM) and selected area electron diffraction (SAED) measurements were performed on a JEM-2100 electron microscope operated at 80 kV. The X-ray diffraction (XRD) patterns were measured by a D/max 2400 X -ray diffractometer with

Cu Kα radiation (λ = 1.54050 Å) operated in the 2θ range from 3 to 40°. The photoluminescence (PL) and absorption spectra of the samples were measured on ultraviolet and visible spectrophotometer (HATCHI U3600H) and fluorescence spectrophotometer (HATCHI F4600). The fluorescence microscopy images were obtained using fluorescence microscopy (Olympus FV1000-IX81) with a spot-enhanced charged couple device (CCD, Diagnostic Instrument, Inc.). Moreover, the steady-state and temperature dependent PL spectra, PL quantum yield (PLQY, Φ), and lifetime (τ) were measured on an Edinburgh steady-state transient fluorescence spectrometer (FLS1000). The samples were both deposited on the surface of a cover glass substrate.

Calculation details: Density functional theory (DFT) and time-dependent DFT (TD-DFT) for 3- and 4-BrTC cocrystals were performed based on their single-crystal data with ωB97-XD/def2-TZVP level in Gaussian 09 program package[1]. Using the optDFTω program[2] to optimize the long-range correction functional ω parameter, we obtained the optimal ω parameters and the ω value of 3- and 4-BrTC is estimated to be 0.1829 and 0.1885 $Bohr^{-1}$, respectively. We also calculated the SOC constants of 3- and 4-BrTC cocrystals, which were estimated by employing the Breit-Pauli spin-orbit Hamiltonian with an effective charge approximation implemented in the PySOC code[3].

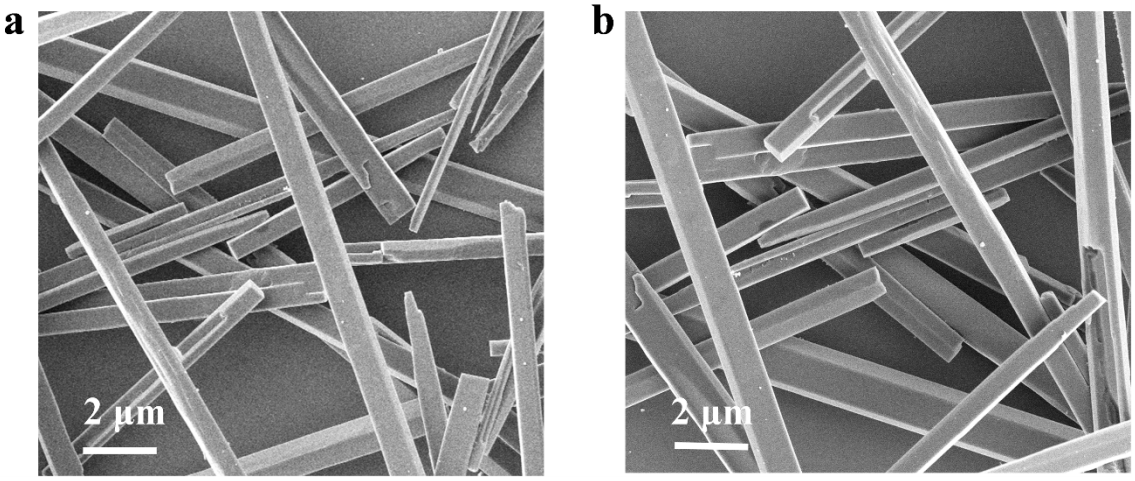

Figure S1. SEM images of (a) 3- and (b) 4-BrTC assemblies. All scale bars are 2 µm.

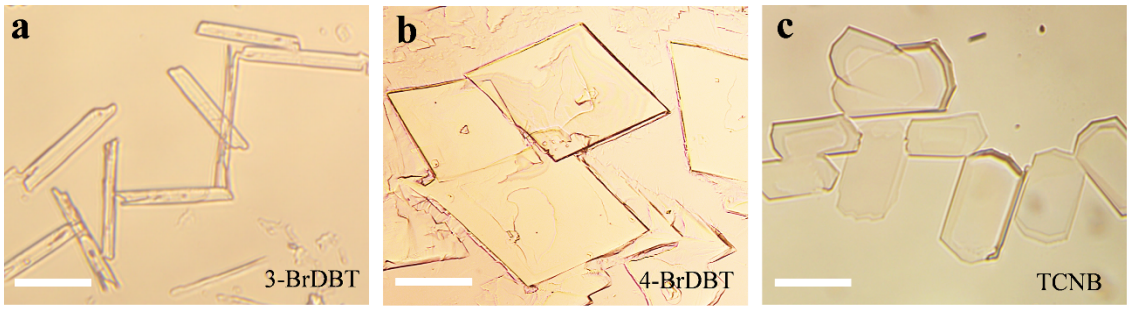

Figure S2. Optical images of 3-BrDBT, 4-BrDBT, and TCNB microcrystals obtained by drop casting of their respective THF solution on the glass substrate. All scale bars are 10 μm.

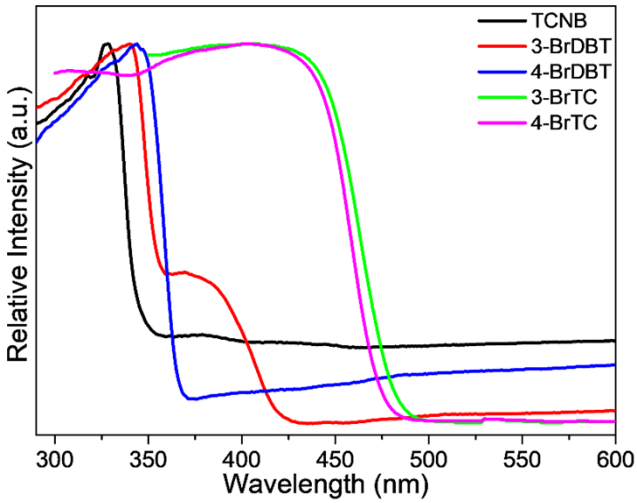

Figure S3. Diffuse reflection absorption spectra of TCNB (black line), 3-BrDBT (red line), and 4-BrDBT microcrystals (blue line) as well as 3- (green line) and 4-BrTC microrods (pink line) at 298 K.

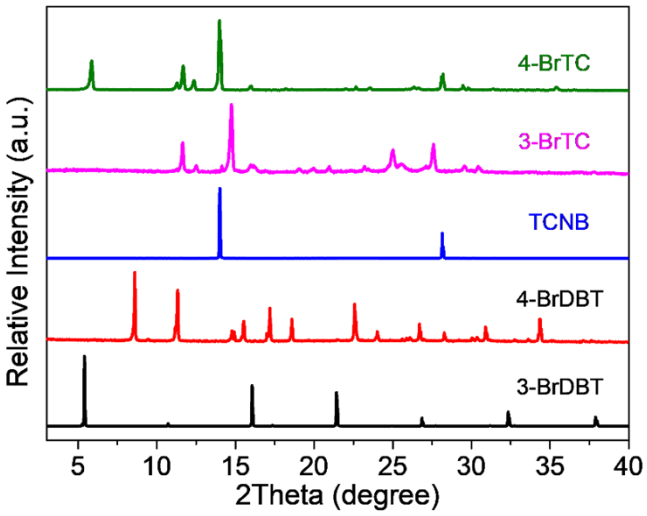

Figure S4. PXRD patterns of 3-BrDBT (black line), 4-BrDBT (red line), and TCNB microcrystals (blue line) as well as 3- (pink line) and 4-BrTC microrods (green line).

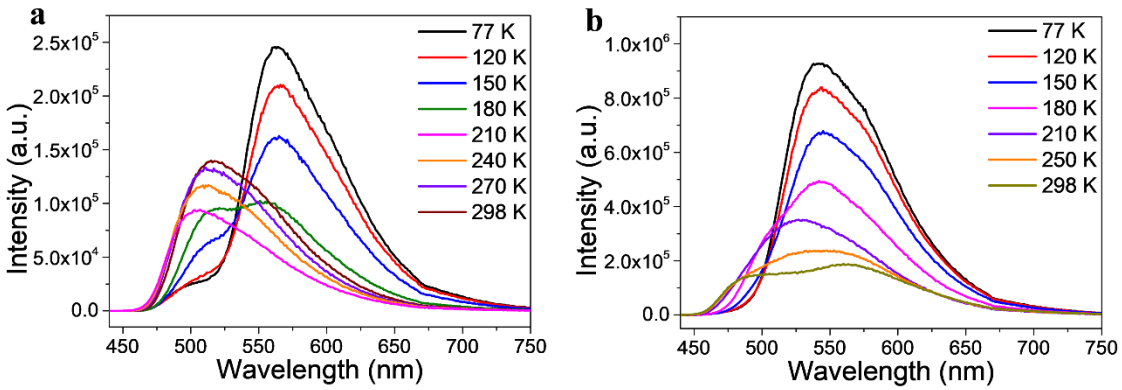

Figure S5. Variable temperature PL spectra of 3- (a) and 4-BrTC microrods (b) ranging from 77 K to 298 K.

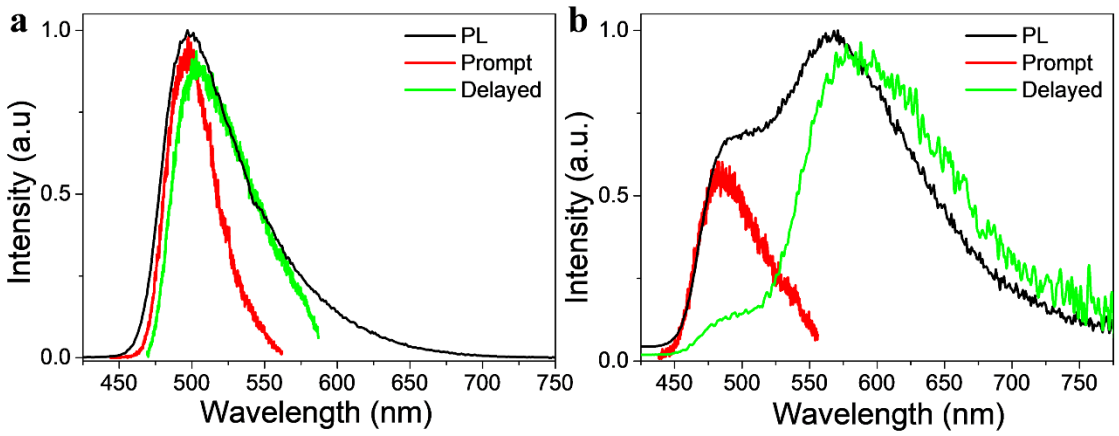

Figure S6. Steady-state (black line), prompt (red line) and delayed PL (green line) spectra of 3-(a) and 4-BrTC microrods (b) at 298 K.

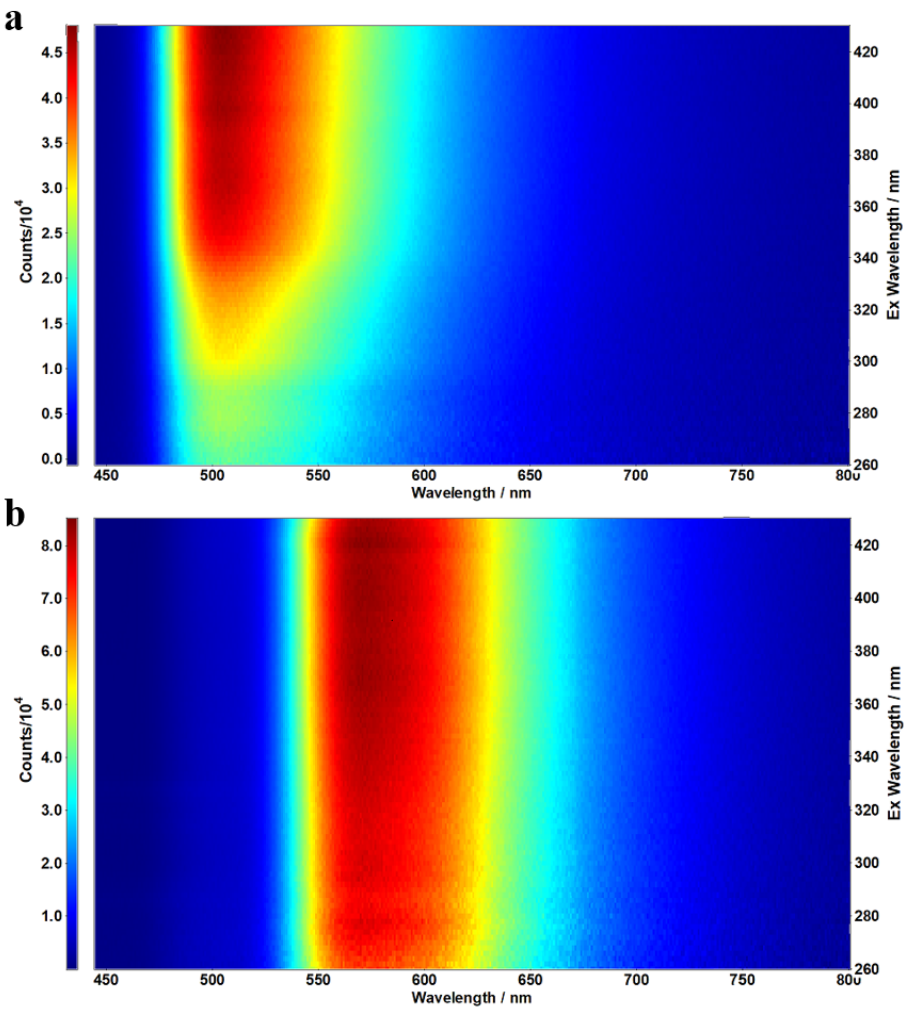

Figure S7. (a, b) Excitation-dependent emission mapping spectra of 3-BrTC at 298 K (a) and 77 K (b), respectively.

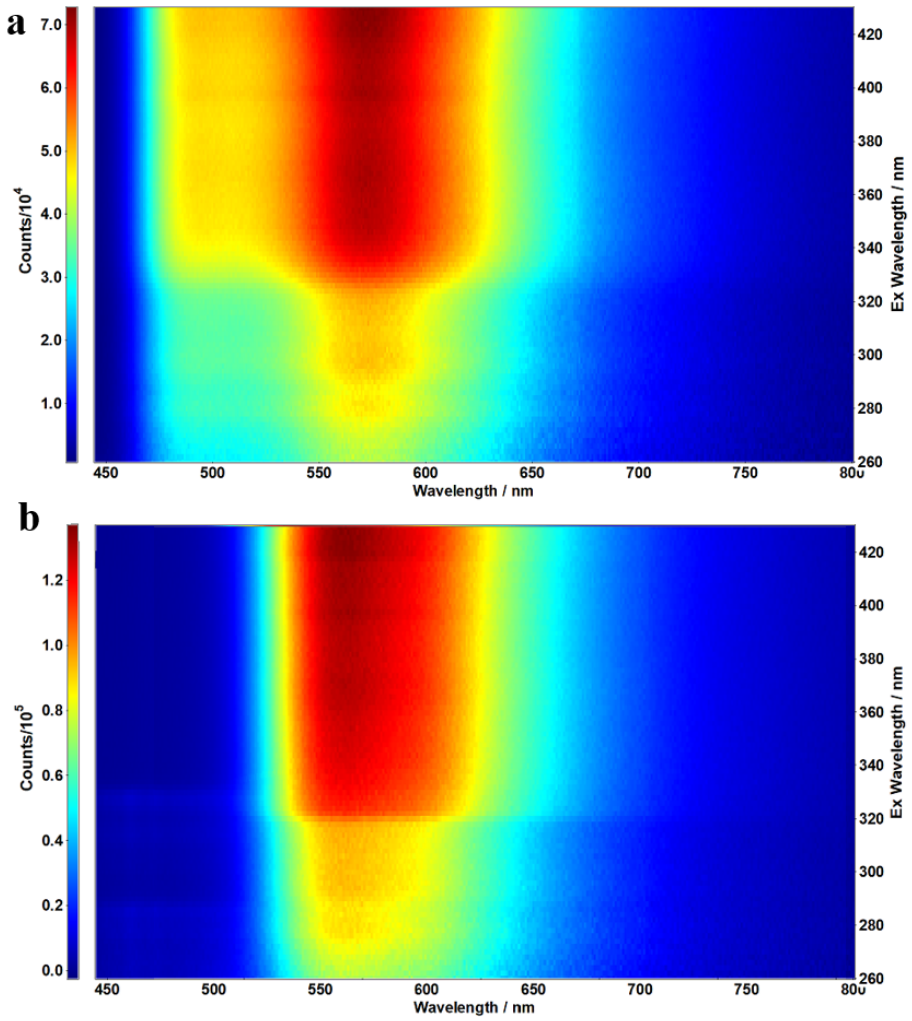

Figure S8. (a, b) Excitation-dependent emission mapping spectra of 4-BrTC at 298 K (a) and 77 K (b), respectively.

Table S1. Crystallographic parameters of 3- and 4-BrTC cocrystals

Identification code	3-BrTC	4-BrTC
Empirical formula	$C_{22}H_9BrN_4S$	$C_{22}H_9BrN_4S$
Formula weight	441.30	441.30
Crystal system	triclinic	monoclinic
Space group	P -1	P 2(1)/c
a/Å	7.5508(15)	7.4921(15)
b/Å	8.0138(16)	8.1212(16)
c/Å	8.1390(16)	30.277(6)
α/°	85.38(3)	90
β/°	77.75(3)	92.33(3)
γ/°	75.07(3)	90
Volume/Å^3	464.86(18)	1840.6(6)
Z	1	4
ρcalc/(g/cm^3)	1.576	1.592

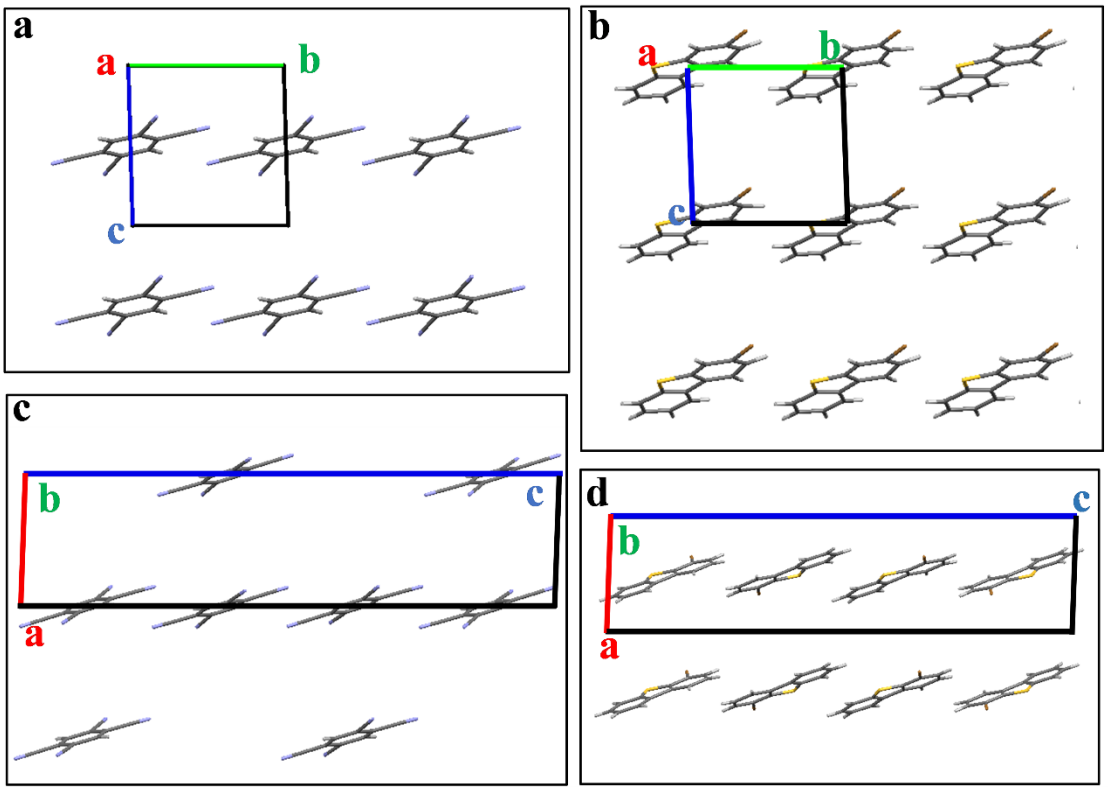

Figure S9. (a-b) Molecular packing structures of TCNB (a) and 3-BrDBT (b) in cocrystal 3-BrTC. (c-d) Molecular packing structures of TCNB (c) and 4-BrDBT (d) in cocrystal 4-BrTC.

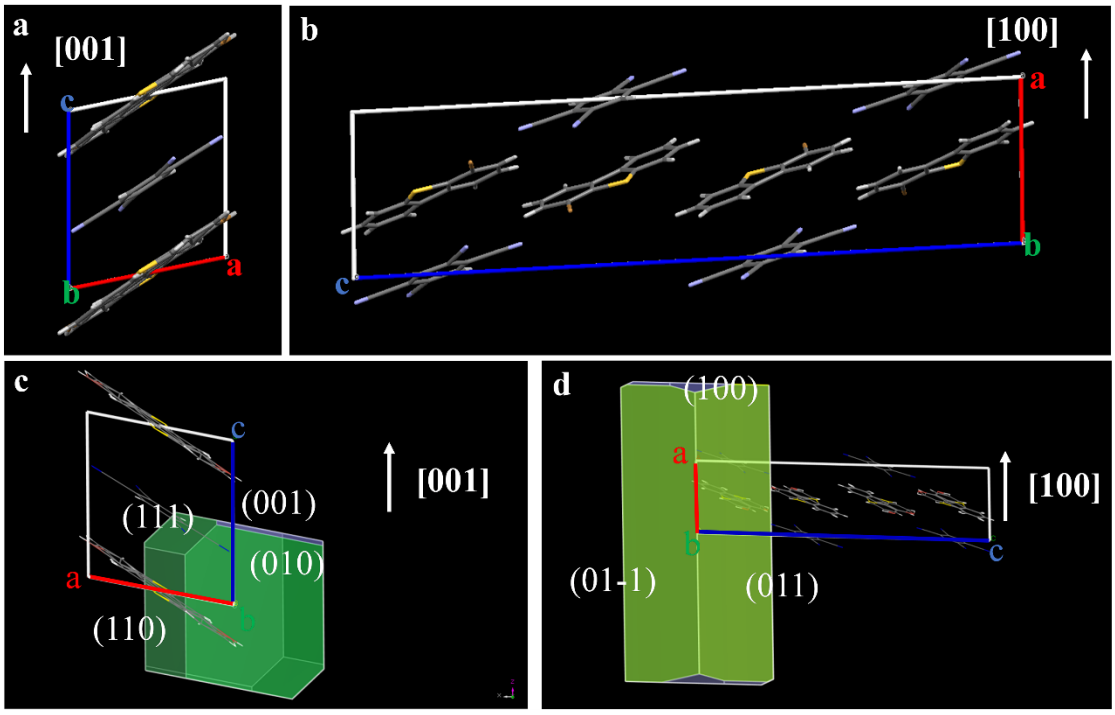

Figure S10. (a-b) Predicted growth morphologies of 3- and 4-BrTC cocrystals simulated using Material Studio software. (c-d) Molecular packing of (c) 3- and (d) 4-BrTC cocrystals along the growth direction, respectively.

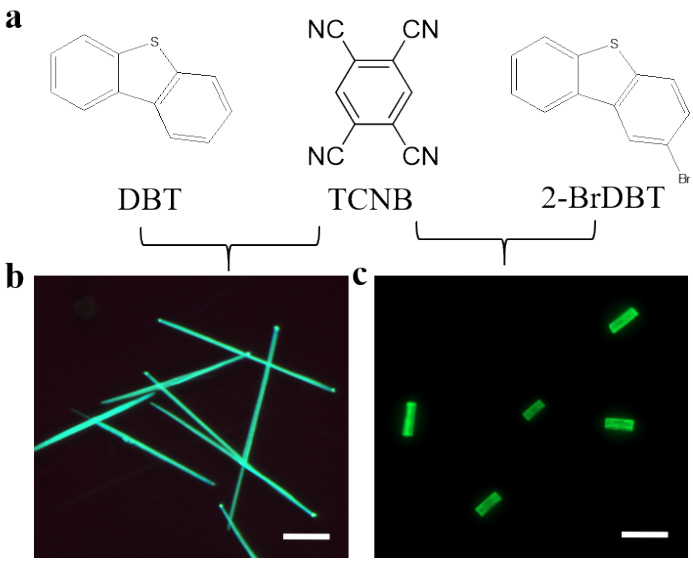

Figure S11. (a) Molecular structures of DBT, TCNB, and 2-BrDBT. (b, c) Fluorescence microscopy images of (b) DTC and (c) 2-BrTC assemblies under 365 nm UV light. All scale bars are 10 μm.

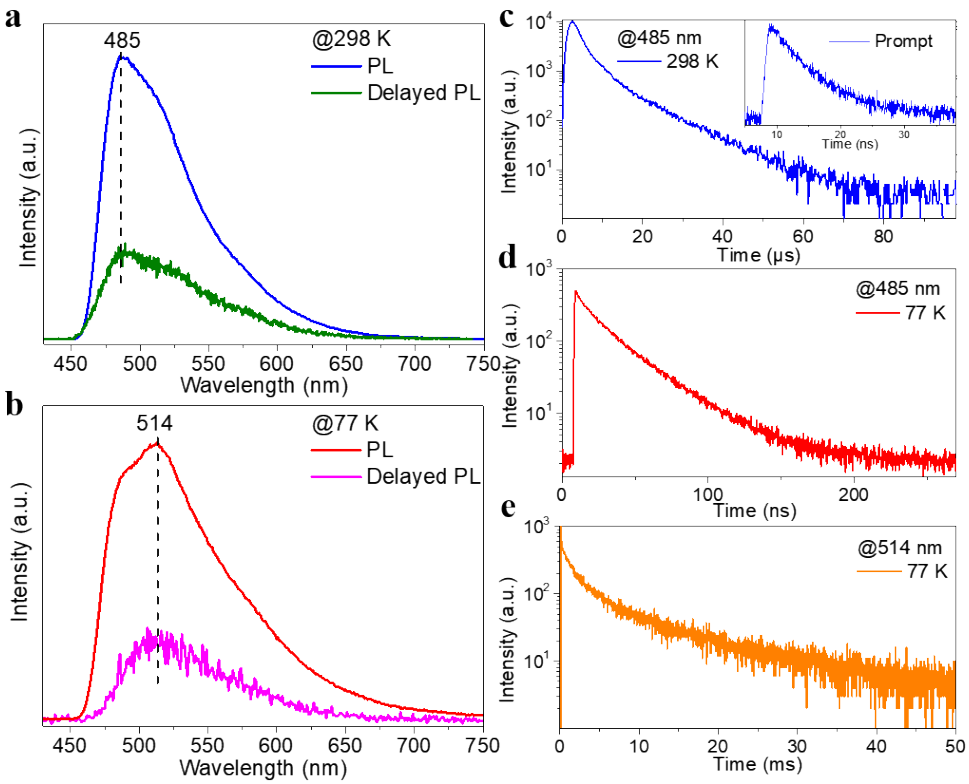

Figure S12. (a, b) Steady-state (blue line) and delayed PL (green line) spectra of DTC microrods at 298 K (a) and 77 K (b). (c) The PL decay curves at 485 nm of DTC at 298 K. (d, e) The PL decay curves line at 485 nm (d) and 514 nm (e) of DTC at 77 K，respectively.

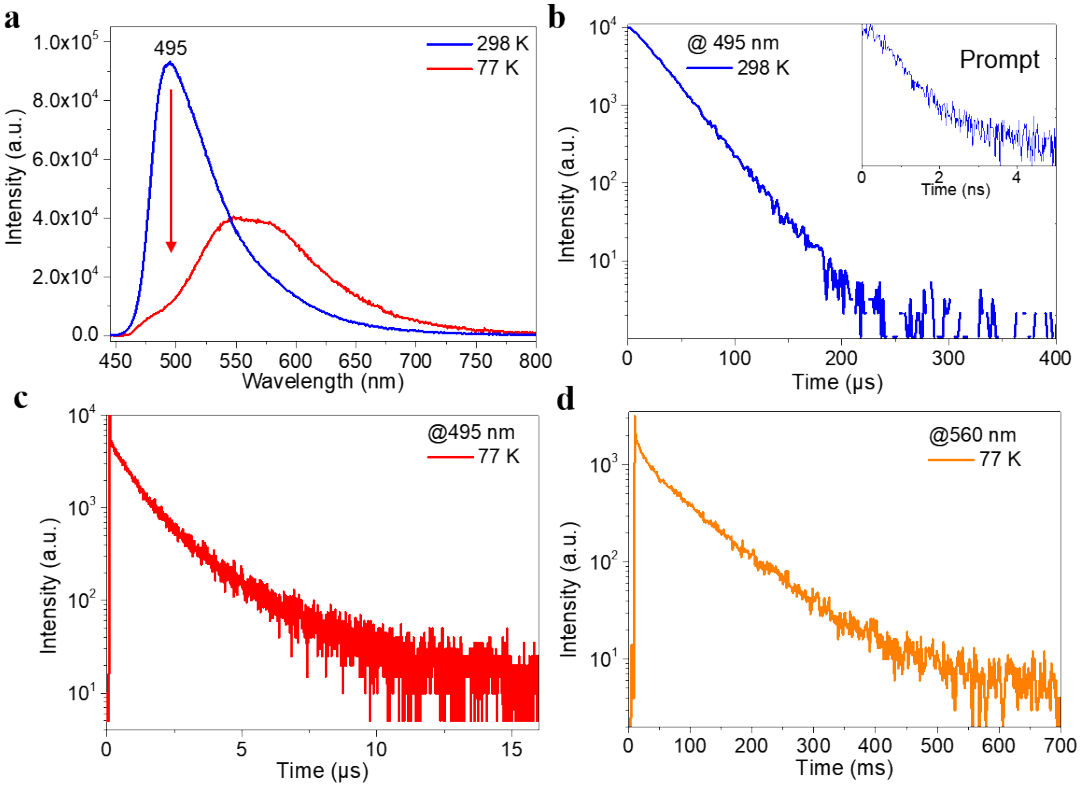

Figure S13. (a) Variable temperature PL spectra of 2-BrTC at 298 K (blue line) and 77 K (red line). (b) The PL decay curves at 495 nm of 2-BrTC at 298 K. (c, d) The PL decay curves at 495 nm (c) and 560 nm (d) of 2-BrTC at 77 K.

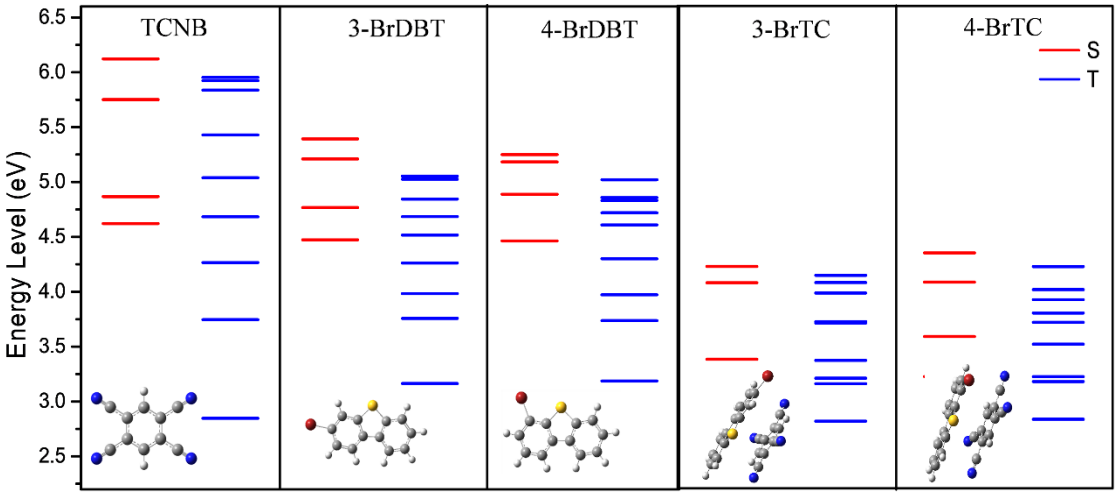

Figure S14. Energy level diagrams of TCNB, 3-BrDBT, and 4-BrDBT as well as 3- and 4-BrTC.

Table S2. Optimized optimal ω parameter of 3-BrTC.

ω	**J**	**J^2**
0.219959	0.0111501300	0.0000621925
0.155041	0.0102124700	0.0000521908
0.184541	0.0005192400	0.0000001357
0.186078	0.0010447300	0.0000005461
0.183270	0.0001154100	0.0000000076
0.183056	0.0000497900	0.0000000023
0.182918	0.0000482700	0.0000000013
0.182900	0.0000482700	0.0000000013
0.182882	0.0000482700	0.0000000013
0.172247	0.0037211600	0.0000069322
0.178820	0.0014042600	0.0000009899
0.181330	0.0005504200	0.0000001530
0.182289	0.0002126000	0.0000000241
0.182655	0.0000814100	0.0000000046
0.182795	0.0000536100	0.0000000024
0.182849	0.0000536100	0.0000000024
The final ω: 0.182882 $Bohr^{-1}$ J^2: 0.0000000013		

Table S3. Optimized optimal ω parameter of 4-BrTC.

ω	**J**	**J^2**
0.219959	0.0093850700	0.0000446472
0.155041	0.0121582500	0.0000740174
0.195629	0.0022550400	0.0000029375
0.191737	0.0010223000	0.0000008768
0.187378	0.0008070600	0.0000003977
0.188477	0.0008102100	0.0000003283
0.188522	0.0008102100	0.0000003283
0.188541	0.0008102100	0.0000003283
0.189762	0.0008243600	0.0000004264
0.189008	0.0008187900	0.0000003466
0.188719	0.0008116400	0.0000003310
0.188609	0.0008159300	0.0000003330
0.188567	0.0008159300	0.0000003330
The final ω: 0.188541 $Bohr^{-1}$ J^2: 0.0000003283		

Table S4. The singlet and triplet excited state transition configurations of 3-BrTC revealed by TD-DFT calculations. Transitions containing n components were highlighted in red.

	Energy (eV)	Transition configuration (%)
S_1	3.2048	H→L (98.4)
T_1	2.8137	H-6→L+1 (13.3) , H-5→L (6.4) , H-4→L (38.7) , H-3→L (2.8) , H-2→L (5.3) , H→L (5.8)
T_2	3.1547	H-1→L +2 (25.0), H→L (54.1), H→L+4 (4.7)
T_3	3.2047	H-3→L+8 (2.3) , H-2→L+3 (5.3) , H-1→ L+2 (38.8), H→L (36.0) , H→L+3 (5.7)
T_4	3.3676	H-1→L (93.4)

Table S5. The singlet and triplet excited state transition configurations of 4-BrTC revealed by TD-DFT calculations. Transitions containing n components were highlighted in red.

	Energy (eV)	Transition configuration (%)
S_1	3.2192	H→L (98.4)
T_1	2.8305	H-6→L+1 (16.8) , H-5→L (21.7) , H-4→L (19.7) , H-3→L (26.8) , H-2→L (6.8)
T_2	3.1741	H-1→L+2 (15.4), H→L (72.9), H→L+4 (2.7)
T_3	3.2188	H-2→L+3 (3.3) , H-1→ L+2 (48.2) , H→L (22.2) , H→L+3 (8.1) , H→L+4 (4.1)
T_4	3.5153	H-6→L (5.4), H-1→ L (88.8)

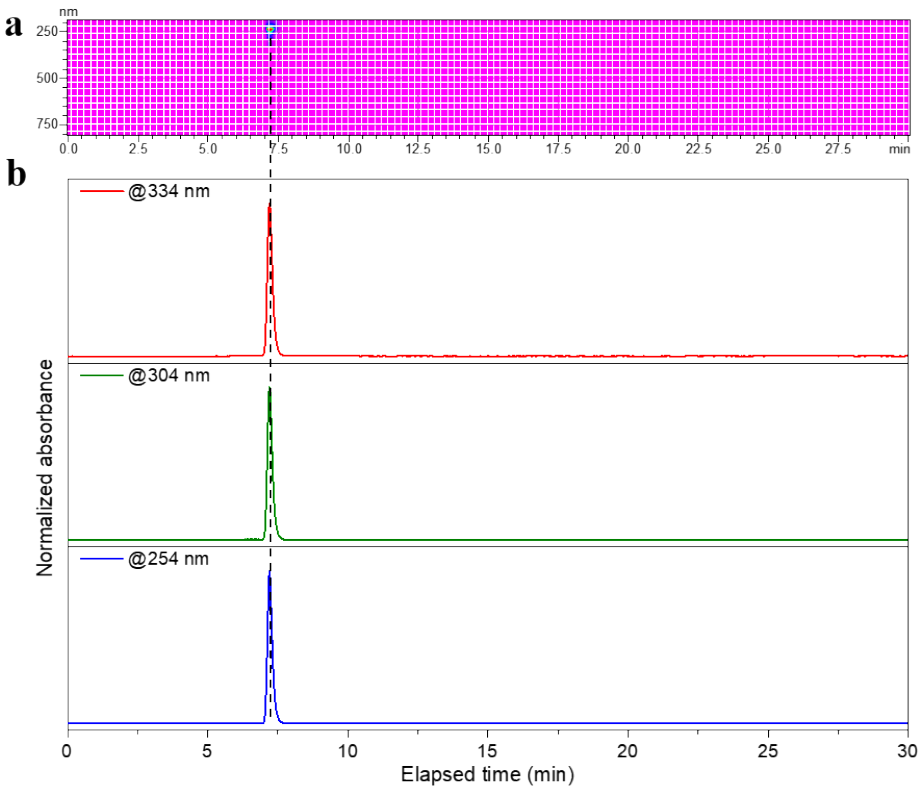

Figure S15. HPLC analysis (a, b) for DBT with Cosmosil 5C18-MS-II column. Chromatographic conditions: flow rate = 0.5 mL/min, eluent = methanol/dichloromethane (v/v= 50/50), column temperature = 25 °C, monitored at different wavelengths.

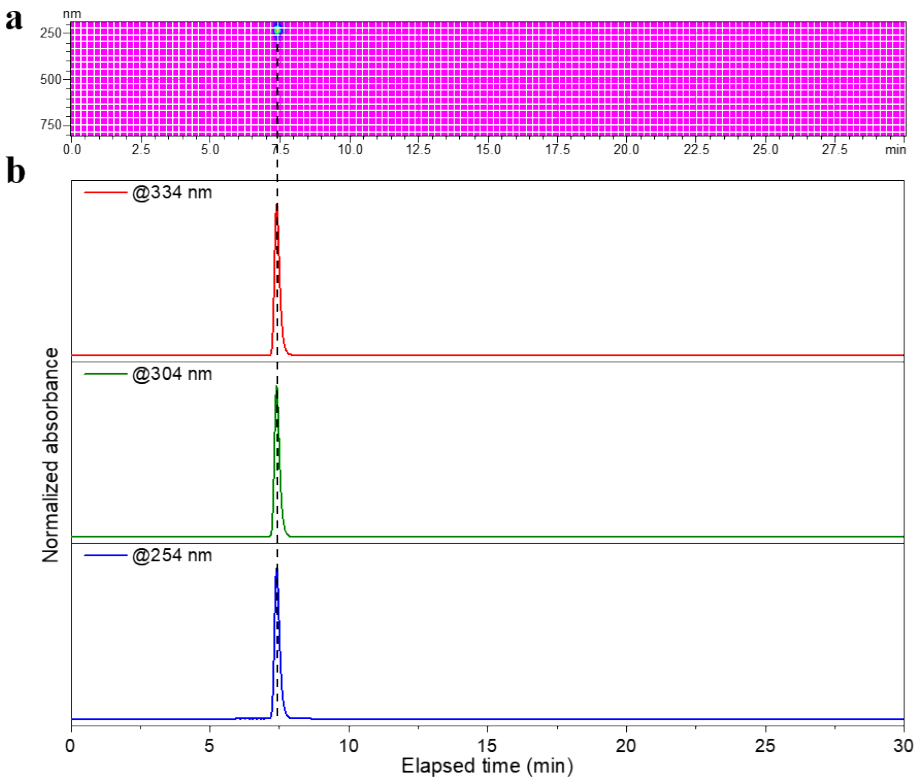

Figure S16. HPLC analysis (a, b) for 2-BrDBT with Cosmosil 5C18-MS-II column. Chromatographic conditions: flow rate = 0.5 mL/min, eluent = methanol/dichloromethane (v/v= 50/50), column temperature = 25 °C, monitored at different wavelengths.

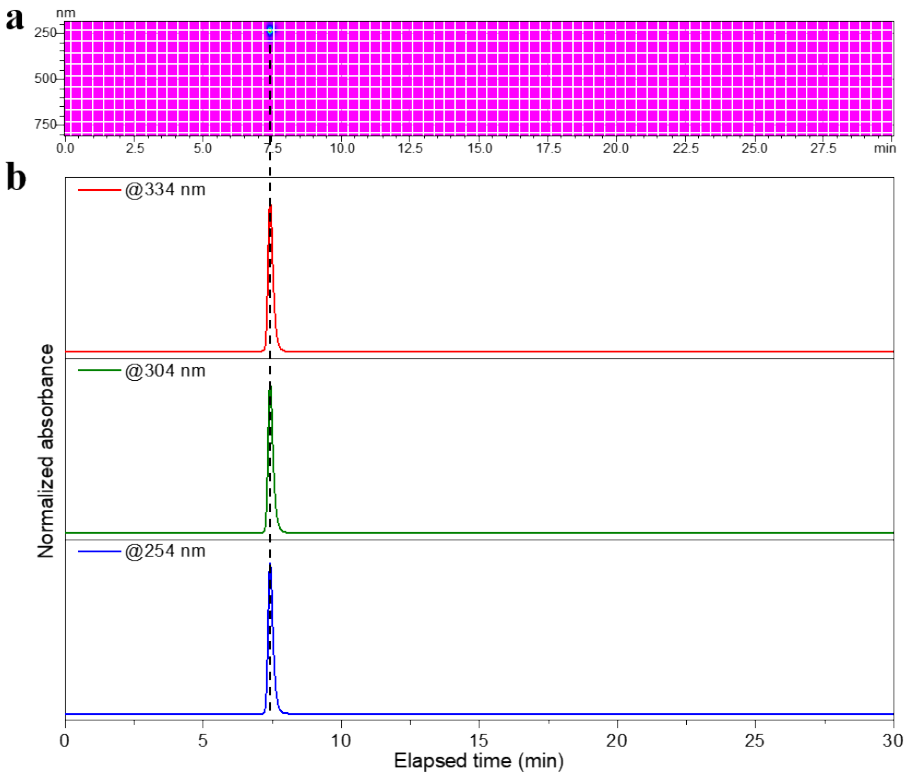

Figure S17. HPLC analysis (a, b) for 3-BrDBT with Cosmosil 5C18-MS-II column. Chromatographic conditions: flow rate = 0.5 mL/min, eluent = methanol/dichloromethane (v/v= 50/50), column temperature = 25 °C, monitored at different wavelengths.

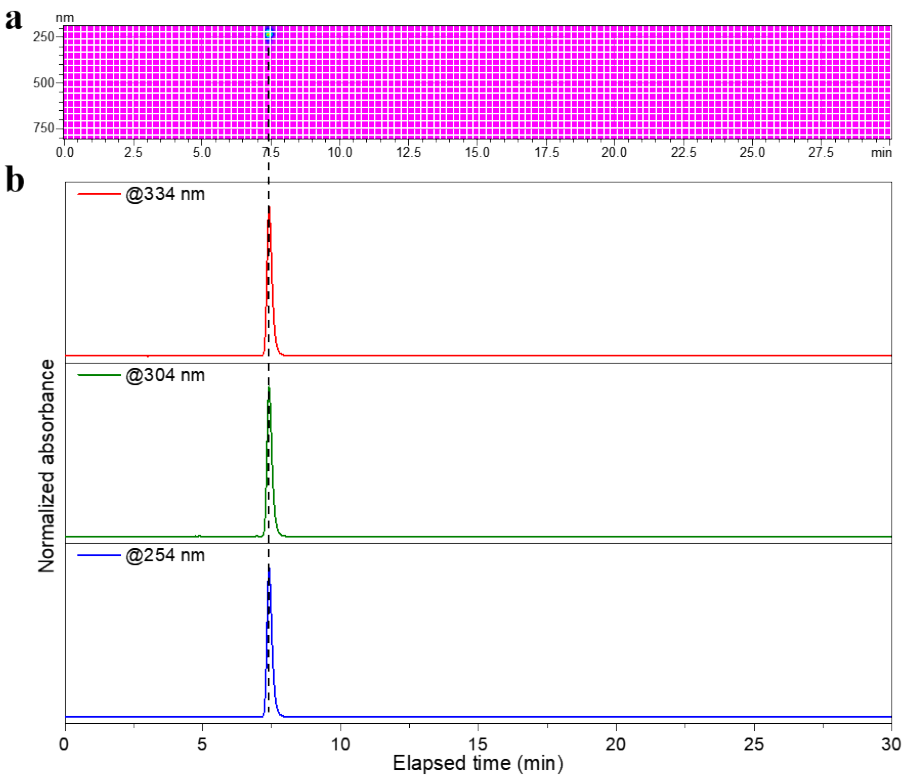

Figure S18. HPLC analysis (a, b) for 4-BrDBT with Cosmosil 5C18-MS-II column. Chromatographic conditions: flow rate = 0.5 mL/min, eluent = methanol/dichloromethane (v/v= 50/50), column temperature = 25 °C, monitored at different wavelengths.

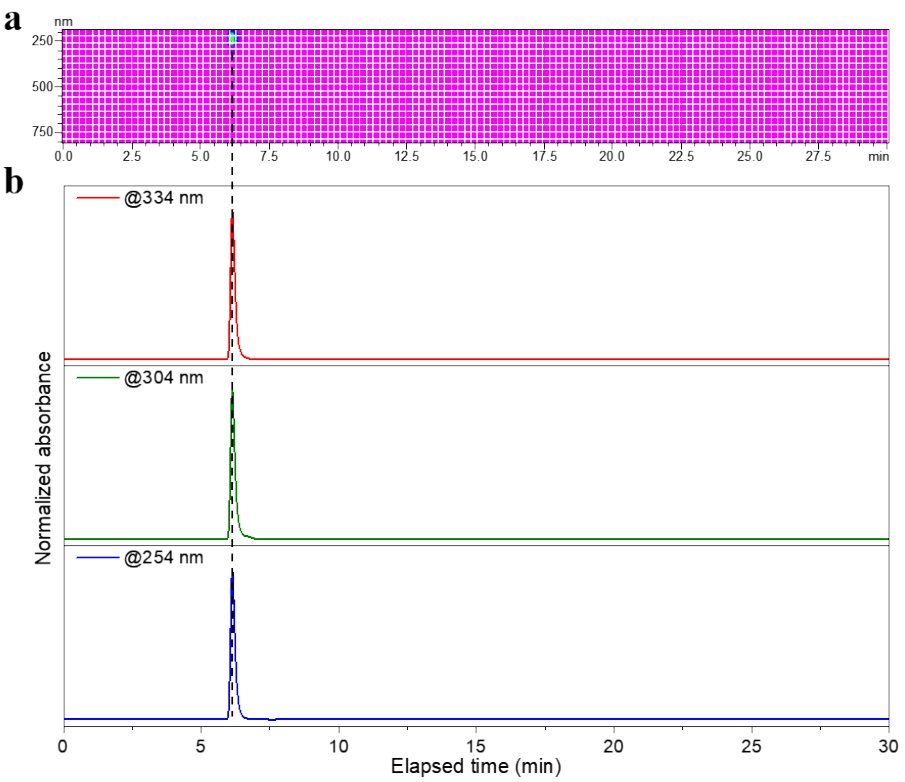

Figure S19. HPLC analysis (a, b) for TCNB with Cosmosil 5C18-MS-II column. Chromatographic conditions: flow rate = 0.5 mL/min, eluent = methanol/dichloromethane (v/v= 50/50), column temperature = 25 °C, monitored at different wavelengths.

References

1. M. J. Frisch, G. W. Trucks, H. B. Schlegel, G. E. Scuseria, M. A. Robb, J. R. Cheeseman, G. Scalmani, V. Barone, B. Mennucci, G. A. Petersson, H. Nakatsuji, M. Caricato, X. Li, H. P. Hratchian, A. F. Izmaylov, J. Bloino, G. Zheng, J. L. Sonnenberg, M. Hada, M. Ehara, K. Toyota, R. Fukuda, J. Hasegawa, M. Ishida, T. Nakajima, Y. Honda, O. Kitao, H. Nakai, T. Vreven, J. Montgomery, A. Jr., J. E. Peralta, F. Ogliaro, M. Bearpark, J. J. Heyd, E. Brothers, K. N. Kudin, V. N. Staroverov, R. Kobayashi, J. Normand, K. Raghavachari, A. Rendell, J. C. Burant, S. S. Iyengar, J. Tomasi, M. Cossi, N. Rega, J. M. Millam, M. Klene, J. E. Knox, J. B. Cross, V. Bakken, C. Adamo, J. Jaramillo, R. Gomperts, R. E. Stratmann, O. Yazyev, A. J. Austin, R. Cammi, C. Pomelli, J. W. Ochterski, R. L. Martin, K. Morokuma, V. G. Zakrzewski, G. A. Voth, P. Salvador, J. J. Dannenberg, S. Dapprich, A. D. Daniels, Ö. Farkas, J. B. Foresman, J. V. Ortiz, J. Cioslowski and D. J. Fox, Gaussian Inc., Wallingford CT, 2009.

2. L. Tian, optDFTω program v1.0.

3. X. Gao, S. Bai, D. Fazzi, T. Niehaus, M. Barbatti and W. Thiel, *J. Chem. Theory Comput*, 2017, **13**, 515.